Chemical Physics Letters 701 (2018) 115–125

Contents lists available at ScienceDirect

Chemical Physics Letters

journal homepage: www.elsevier.com/locate/cplett

Research paper

Temperature dependent selective detection of hydrogen and acetone using Pd doped WO_3/reduced graphene oxide nanocomposite

Jasmeet Kaur, Kanica Anand, Nipin Kohli, Amanpreet Kaur, Ravi Chand Singh *

Department of Physics, Guru Nanak Dev University, Amritsar 143005, Punjab, India

ARTICLE INFO

Article history:
Received 30 January 2018
In final form 23 April 2018
Available online 24 April 2018

Keywords:
Gas sensor
Temperature dependent selectivity
Reduced graphene oxide
WO_3
Pd doping

ABSTRACT

Reduced graphene oxide (RGO) and Pd doped WO_3 nanocomposites were fabricated by employing electrostatic interactions between poly (diallyldimethylammonium chloride) (PDDA) modified Pd doped WO_3 nanostructures and graphite oxide (GO) and studied for their gas sensing application. XRD, Raman, FTIR, FESEM-EDX, TEM, TGA, XPS and Photoluminescence techniques were used for characterization of as-synthesized samples. Gas sensing studies revealed that the sensor with optimized doping of 1.5 mol% Pd and 1 wt% GO shows temperature dependent selectivity towards hydrogen and acetone. The role of WO_3, Pd and RGO has been discussed in detail for enhanced sensing performance.

1. Introduction

In recent years, metal oxide semiconductors have gained significant attention in gas sensing area for detecting various gases including hydrogen (H_2) and acetone. Among these metal oxides, tungsten trioxide (WO_3), an n-type semiconductor, has been considered as one of the promising material for gas sensing application due to its noteworthy role in detection of reducing/oxidizing gases, low cost, and for being environment-friendly [1–5]. However, the practical applicability of WO_3 sensor suffers major drawbacks such as poor selectivity and high operating temperatures which leads to excessive power consumption and deterioration of the sample.

In order to overcome these limitations and to improve the gas sensing performance, recent research has been motivated by realizing the importance of noble metals or carbon materials and hybridization of these materials with metal-oxide semiconductor sensors. The presence of noble metal, whether as a catalyst or as a dopant, alter the specific surface area, activation energy and the bulk resistance of metal oxides which eventually offers improved sensing properties [6]. Due to its excellent chemical, electronic and mechanical properties, the incorporation of reduced graphene oxide (RGO) also enhances sensing properties of metal-oxides synergically. RGO provide large specific surface area, high conductivity, and electron acceptor ability to hike the sensing properties [7].

In this paper, we are reporting the possibility of hybridizing the advantages of RGO sheets along with merits of Pd doping in WO_3 nanostructures for temperature dependent selective detection of hydrogen (H_2) and acetone. It is a well-known fact that H_2 is one of the promising clean and renewable energy sources and is extensively employed in industries, fuel for power generation and transportation, etc [8]. Due to its colorless, odorless and inflammable nature, the demand for early detection of H_2 is extremely important. Palladium (Pd) is one of the best choices for H_2 sensing due to its extraordinary sticking and diffusion coefficient for H_2 [9]. The catalytic dissociation capability of Pd also contributes to excellent sensitivity [6].

Recently, the hybridization of doped metal oxide semiconductors and RGO has emerged as an innovative approach to improve the overall sensing properties of gas sensors [10]. For example, Esfandiar et al. recently reported Pd doped WO_3/RGO nanocomposites for the detection of hydrogen [11]. Su et al. reported Pd/SnO_2/RGO ternary composite for room temperature NH_3 sensing [12]. Toloman et al. also investigated humidity sensing properties of RGO decorated with Fe doped SnO_2 nanoparticles [13]. Recently, our group reported gadolinium doped WO_3 and RGO nanocomposite for acetone detection [14]. To the best of our knowledge, there are no reports available in literature on temperature dependent selective behaviour based on Pd doped WO_3 nanostructures and RGO nanocomposites towards H_2 and acetone. To accomplish this, first of all, pure and Pd doped (0.5, 1.0 and 1.5 mol%) WO_3 nanostructures were synthesized using simple acid precipitation method and subsequently studied for gas sensing application. The sensor based on optimum doping amount of Pd doping i.e. 1.5 mol% has

---

* Corresponding author.
E-mail address: rc.phy@gndu.ac.in (R.C. Singh).

https://doi.org/10.1016/j.cplett.2018.04.049
0009-2614/

exhibited temperature dependent selective behaviour. Further improvement in sensing response and reduction in working temperature has been achieved by incorporating RGO. The role of Pd doping and RGO incorporation on enhanced gas sensing performance of WO_3 nanostructures has been discussed in detail.

2. Experimental

The materials used in this work are given in supplementary material (see S2.1). Methodology used to prepare pure WO_3, Pd doped WO_3 and RGO based nanocomposites is same as described in our previous work reported elsewhere [14]. However, detail synthesis process can be found in supplementary material (see S2.2). Room temperature acid precipitation was used to prepare pure and Pd doped WO_3 nanostructures where $Na_2WO_4{\cdot}2H_2O$ and $PdCl_2$ were the precursors of WO_3 and Pd, respectively. Different concentrations of Pd (0.5, 1.0 and 1.5 mol%) were used and labeled as Pd0.5, Pd1.0, and Pd1.5, respectively. Graphite oxide (GO) was synthesized by means of modified Hummer's method [15]. The attachment of Pd1.5 on to RGO sheets was attained by electrostatic interactions by using PDDA. Samples with different concentration of GO (0.5, 1.0 and 2.0 wt%) were labelled as PdG0.5, PdG1.0 and PdG2.0, respectively.

The details of all characterization techniques and gas sensing measurements are given in supplementary material (see S2.3).

3. Results and discussion

3.1. Characterization of as-synthesized samples

The XRD spectra of WO_3 and Pd doped WO_3 nanostructures are displayed in Fig. 1a. The presence of three strong peaks versus 2θ ranging from 22 to 25° correspond to reflection planes (2 0 0), (0 2 0) and (0 0 2) indicating the monoclinic phase of WO_3 nanostructures which is consistent with standard data (JCPDS-83-0951) [16]. In Pd doped WO_3 samples, no peak related to Pd appears in XRD patterns which may be attributed to successful incorporation of Pd into the WO_3 lattice. The intensity of diffraction peaks also decreases with Pd doping which arises from lattice distortion induced by Pd as the ionic radius of host ion is smaller (ionic radii of W^{6+} and Pd^{2+} are 67 and 78 pm respectively) than dopant ion [17]. The average crystallite size (D) has been estimated using Scherrer's equation [18] by considering triplet peaks (2 0 0), (0 2 0) and (0 0 2) and the obtained values are 28.70, 18.89, 19.79, and 18.04 nm for pure WO_3, Pd0.5, Pd1.0, and Pd1.5 respectively. The average crystallite size decreases with Pd doping implying that incorporation of Pd restrains the growth of WO_3 nanostructures which is beneficial in improving sensing performance. Similar reduction in crystallite size on doping has been reported in literature [14,19].

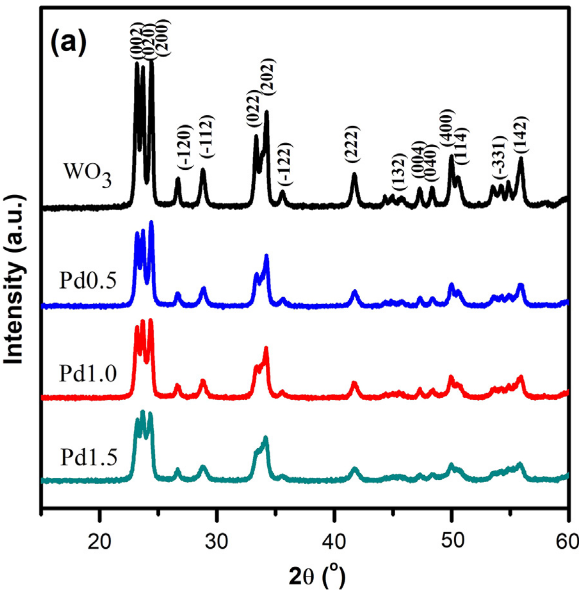

Fig. 1a. XRD patterns of pure and Pd doped WO_3 nanostructures.

We also performed Rietveld refinements on XRD data of pure and Pd doped WO_3 samples with Full Prof program using P 21/n space group. The refined XRD patterns are shown in Fig. 1b and the lattice parameters ('a', 'b', 'c' and 'β' and Chi-square values) extracted from Rietveld analysis are displayed in Table S1 (see supplementary material). Upadhyay et al. have observed similar variations in lattice parameters and cell volume in case of indium doped WO_3 [16] and have attributed this deviation to presence of dopant in WO_3 lattice.

The XRD patterns of GO and RGO are displayed in Fig. 1c, showing a prominent peak at 2θ = 10.90° for GO corresponding to (0 0 1) reflection of graphite oxide. This peak vanishes after reduction of GO into RGO [20]. The RGO based nanocomposites exhibit XRD patterns (Fig. 1c) similar to monoclinic WO_3. No peaks corresponding to Pd, GO or RGO were detected in nanocomposite which may be attributed to their low content and proper exfoliation of RGO sheets [21,22].

Fig. 2a depicts the Raman spectra of pure and Pd doped WO_3 nanostructures. Raman spectrum of pure WO_3 shows the presence of W-O-W stretching (808 and 715 cm^{-1}) and O-W-O bending vibration modes (327 and 275 cm^{-1}) [16]. The effect of Pd dopant can be seen by slight broadening and shifting of above bands, thus confirming the incorporation of Pd into host lattice. The Pd doped WO_3 nanostructures also exhibited a reduction in intensity in comparison to pure WO_3 which is ascribed to the existence of structural disorder that originates upon doping [19].

Fig. 2b displays the Raman spectra of GO, RGO and RGO based nanocomposites. It is observed that GO displays two notable D and G bands at around 1358 and 1604 cm^{-1}. The D band is ascribed to sp^3- hybridized carbon and presence of defects, whereas, G band is accredited to first-order scattering of E_{2g} phonons of sp^2 carbon atoms [23]. These bands are also present in RGO and nanocomposites but with slight shifting towards lower wavenumbers. The typical bands of WO_3 are also present in nanocomposites. Besides this, we also measured the intensity ratio of D and G bands (I_D/I_G) which shows an increase in its value for RGO and nanocomposites in comparison to GO. In general, the higher ratio of I_D/I_G signifies the degree of defects and disorder in graphitic materials and presence of these defects boosts the adsorption of oxygen and gas species which could be beneficial in improving gas sensing response [24].

The FTIR spectra of WO_3, Pd1.5, GO, and PdG1.0 are shown in Fig. 3a. The spectrum of GO shows a broad band at 3444 cm^{-1} and is attributed to O—H stretching vibrations. The characteristic absorption band of C=C stretching vibration is found at 1643 cm^{-1} whereas the peak present at 1741 cm^{-1} is related to COOH stretching vibrations. The intensity of O—H absorption band decreases in RGO based nanocomposite, thus confirming the successful reduction of RGO. The other absorption bands at 1741, 1371 and 1085 cm^{-1} are attributed to a typical stretching vibration of —C=O (carboxyl), deformation vibration of OH and stretching vibration of —C—O (alkoxy), respectively [25]. Except GO, in all other three samples, the bands below 1000 cm^{-1} are associated with stretching vibrations of WO_3 [26]. However, with Pd doping, a frequency shift towards lower side related to these W-O-W stretching vibrations (Fig. 3b) has been observed, suggesting the successful substitution of Pd into the WO_3 lattice [27]. Moreover, it is to be noted that in case of RGO based nanocomposite